Applied Mathematics, 2026, 17(6), 380-391
https://www.scirp.org/journal/am
ISSN Online: 2152-7393
ISSN Print: 2152-7385

An Extended SI-Based SEIQRD Dynamical Model of Infectious Diseases

Zixuan Liao

Guangdong Experimental High School, Guangzhou, China
Email: 13910921634@139.com

How to cite this paper: Liao, Z.X. (2026) An Extended SI-Based SEIQRD Dynamical Model of Infectious Diseases. *Applied Mathematics*, **17**, 380-391.
https://doi.org/10.4236/am.2026.176024

Received: May 6, 2026
Accepted: June 21, 2026
Published: June 24, 2026

Abstract

Infectious disease models are a core tool in mathematical epidemiology, designed to describe, through mathematical equations, the patterns of pathogen transmission within host populations. This paper systematically outlines the development of infectious disease models over the years. After exploring several major factors influencing disease transmission, we introduce new variables into the model and establish the SEIQRD dynamical model based on the SI framework. Using this SEIQRD model, we analyze the transmission of COVID-19 in Wuhan (2022) and New York City (2023). Through the study of the epidemic spread in these two cities, we find that, due to the complexity of the pandemic, the SEIQRD model aligns more closely with actual observations and provides a more accurate description of COVID-19 compared to the earlier SIR model. Furthermore, the experience of managing COVID-19 reveals that, with the continuous advancement of data science, infectious disease modeling is shifting from a macroscopic description of infected populations toward precise predictions of different infection levels and individual infected cases.

Keywords

SEIQRD Model, Infectious Disease Dynamics, Compartmental Model, COVID-19, Quarantine Rate, Quarantine Effectiveness, Sensitivity Analysis

1. Background

Human history has been constantly accompanied by the threat of infectious diseases. From the Black Death in the 14th century to the outbreak of SARS in the early 21st century, and then to the coronavirus disease (COVID-19) that emerged at the end of 2019, each pandemic has inflicted tremendous impacts on human society. In responding to these outbreaks, beyond traditional measures such as isolation and vaccination, mathematical models have gradually become indispensable tools for decision-makers to assess intervention strategies and predict epidemic trends.

The earliest infectious disease model can be traced back to Daniel Bernoulli's study on smallpox inoculation in 1760 [1]. However, the foundational work of modern infectious disease dynamics is generally attributed to two scholars from the early 20th century—Kermack and McKendrick—who proposed the renowned SIR compartmental model in 1927 [2]. This model remains the core framework for all complex models to this day.

This paper aims to comprehensively review the development of infectious disease models, introduce the evolutionary logic from classical models to modern frontiers, and explore their practical value in real-world applications.

Building upon the classical SIR model and considering differences in disease transmission mechanisms, prevention and control interventions, and disease outcomes, this paper gradually introduces new compartments to construct five infectious disease dynamical models of increasing complexity. The parameter definitions, compartmental structures, and differential equations for each model are presented in sequence, followed by a discussion of the applicability and limitations of each model.

2. Model Building

2.1. Modeling Approach

Dynamical modeling of infectious diseases serves as an important quantitative tool for understanding pathogen transmission patterns, evaluating the effectiveness of prevention and control measures, and predicting epidemic development trends. The compartmental modeling approach, owing to its clear structure and strong analytical tractability, has become the cornerstone of mathematical modeling in epidemiology. However, real-world infectious disease transmission often exhibits complex heterogeneity and multi-stage characteristics: different diseases have distinct incubation period features; public health interventions (e.g., isolation, quarantine) dynamically alter population contact patterns; and the clinical outcomes of infected individuals include both recovery and death. The classic SIR model, which crudely lumps all removed individuals into a single category and does not account for latent states or intervention mechanisms, struggles to accurately capture these real-world features.

To address modeling needs under different scenarios, researchers often introduce new compartments or adjust parameter structures based on the SIR model, constructing extended models of increasing complexity. However, as the number of compartments increases, the parameter dimensionality and data requirements also rise, leading to changes in model applicability, robustness, and interpretability.

This study focuses on five typical extended models derived from the classic SIR model [3]: the SI model, which includes only susceptible and infectious compartments; the SIR model, comprising susceptible, infectious, and recovered compartments; the SIQR model, which introduces a quarantined compartment to SIR; the

SIQDR model, further distinguishing between recovered and deceased individuals; and the SEIQRD model, which simultaneously includes exposed (latent), quarantined, recovered, and deceased compartments. These five models exhibit a clear hierarchical and progressive relationship in terms of the number of compartments, assumptions, parameter scale, and applicable scenarios.

This paper aims to systematically outline the mathematical structures of the above five models, clarify their differential equation formulations and parameter definitions, and conduct a comparative analysis of each model in terms of modeling assumptions, applicable disease types, data requirements, and limitations. Through this study, we hope to provide a theoretical basis for infectious disease modelers in selecting and constructing models, as well as to lay the groundwork for subsequent parameter estimation and intervention evaluation based on real-world epidemic data.

2.2. Core Methods

Starting from the most basic SI model (which includes only infected and uninfected individuals), this paper successively introduces the recovered, quarantined, deceased, and exposed compartments. This approach allows the model to more closely reflect real-life conditions while maintaining accuracy and strong robustness against disturbances.

2.3. Model Parameters

Table 1. Summary of model parameter symbols, units, and descriptions.

Parameter symbol	Unit	Description
N	Person	Total population
S	Person	Susceptible individuals—not yet infected but can be infected
I	Person	Infectious individuals—already infected
Q	Person	Quarantined/Isolated individuals—infected and subsequently isolated, no longer capable of transmitting the disease
R	Person	Recovered individuals—infected, treated, and recovered, acquiring immunity
E	Person	Exposed individuals—infected but currently in the latent (incubation) period
D	Person	Deceased individuals—not counted in the total population
β	%	Transmission rate
k	/day	Infectivity coefficient of quarantined individuals relative to unquarantined ones ($0 \le k \le 1$, $k = 0$ isolation completely blocks transmission)
σ	%	Latent progression rate (*i.e.*, reciprocal of the incubation period)
δ	%	Quarantine/Isolation rate
γ_I	%	Recovery rate of unquarantined infectious individuals

Continued

γ_Q	%	Recovery rate of quarantined individuals
μ_I	%	Case fatality rate of unquarantined individuals
μ_Q	%	Case fatality rate of quarantined individuals
R_0	Dimensionless	Average number of secondary infections caused by a single infectious individual over the entire infectious period $R_0 = \beta \frac{\frac{1+k\times\delta}{\gamma_Q+\mu_Q}}{\gamma_I+\mu_I+\delta}$

2.4. Model Construction

2.4.1. SI Model

1) Compartment Division:

S: Susceptible individuals

I: Infectious individuals

Total population $N = S + I$

2) Differential Equations:

$$\begin{cases} \frac{\mathrm{d}S}{\mathrm{d}t} = -\beta \frac{SI}{N} \\ \frac{\mathrm{d}I}{\mathrm{d}t} = \beta \frac{SI}{N} \end{cases}$$

2.4.2. SIR Model

1) Compartment Division

S: Susceptible individuals

I: Infectious individuals

R: Removed individuals

2) Differential Equations

$$\begin{cases} \frac{\mathrm{d}S}{\mathrm{d}t} = -\beta \frac{SI}{N} \\ \frac{\mathrm{d}I}{\mathrm{d}t} = \beta \frac{SI}{N} - \gamma \\ \frac{\mathrm{d}R}{\mathrm{d}t} = \gamma I \end{cases}$$

2.4.3. SIQR Model

1) Compartment Division

S: Susceptible individuals

I: Infectious individuals

Q: Quarantined/Isolated individuals

R: Removed individuals

Total population $N = S + I + Q + R$

2) Differential Equations

$$\begin{cases} \dfrac{\mathrm{d}S}{\mathrm{d}t} = -\beta \dfrac{SI}{N} \\ \dfrac{\mathrm{d}I}{\mathrm{d}t} = \beta \dfrac{SI}{N} - (\gamma + \delta) I \\ \dfrac{\mathrm{d}Q}{\mathrm{d}t} = \delta I - \gamma_Q Q \\ \dfrac{\mathrm{d}R}{\mathrm{d}t} = \gamma_I I + \gamma_Q Q \end{cases}$$

2.4.4. SIQRD Model

1) Compartment Division

S: Susceptible individuals

I: Infectious individuals

Q: Quarantined/Isolated individuals

D: Deceased individuals

R: Recovered individuals

Total living population $N_{\text{living}} = S + I + Q + R + D$, since deceased individuals are counted in the total living population, N_{living} is no longer constant.

2) Differential Equations

$$\begin{cases} \dfrac{\mathrm{d}S}{\mathrm{d}t} = -\beta \dfrac{SI}{N} \\ \dfrac{\mathrm{d}I}{\mathrm{d}t} = \beta \dfrac{SI}{N} - (\gamma_I + \mu_I + \delta) I \\ \dfrac{\mathrm{d}Q}{\mathrm{d}t} = \delta I - (\gamma_Q + \mu_Q) Q \\ \dfrac{\mathrm{d}R}{\mathrm{d}t} = \gamma_I I + \gamma_Q Q \\ \dfrac{\mathrm{d}D}{\mathrm{d}t} = \mu_I I + \mu_Q Q \end{cases}$$

2.4.5. SEIQRD Model

1) Compartment Division

S: Susceptible individuals

E: Exposed individuals

I: Infectious individuals

Q: Quarantined/Isolated individuals

R: Recovered individuals

D: Deceased individuals

Total living population $N_{\text{living}} = S + E + I + Q + R$, since deceased individuals D are not counted in the total living population, N_{living} is no longer constant.

R_0 is directly specified from reports; β is back-calculated from the model's R_0 formula in Table 1. β values in the subsequent simulations are effective per-contact transmission probabilities.

2) Differential Equations

$$
\begin{cases}
\dfrac{\mathrm{d}S}{\mathrm{d}t} = -\beta \dfrac{S(I+kQ)}{N} \\
\dfrac{\mathrm{d}E}{\mathrm{d}t} = \beta \dfrac{S(I+kQ)}{N} - \sigma E \\
\dfrac{\mathrm{d}I}{\mathrm{d}t} = \sigma E - (\gamma_I + \mu_I + \delta) I \\
\dfrac{\mathrm{d}Q}{\mathrm{d}t} = \delta I - (\gamma_Q + \mu_Q) Q \\
\dfrac{\mathrm{d}R}{\mathrm{d}t} = \gamma_I I + \gamma_Q Q \\
\dfrac{\mathrm{d}D}{\mathrm{d}t} = \mu_I I + \mu_Q Q
\end{cases}
$$

3. Data Statistics and Calculation

3.1. Data Sources and Preprocessing

For model calibration and validation, we used publicly reported daily time series of new confirmed cases and new deaths for two cities:

Wuhan (2022): Data from Wuhan Municipal Health Commission official website [4], covering the period from January 1, 2022 to March 31, 2022. The dataset includes daily newly confirmed COVID-19 cases and deaths. The data required for the simulation are in Table 2 and Table 3, and the simulation results are shown in Figure 1.

New York City (2023): Data from the NYC Department of Health and Mental Hygiene (via NYC Open Data), covering the period from January 1, 2023 to June 30, 2023. Daily case counts and death counts were extracted [5]. The data required for the simulation are in Table 4 and Table 5, and the simulation results are shown in Figure 2.

3.2. COVID-19 Transmission in Wuhan, 2022

Table 2. Initial parameters and basic reproduction number for COVID-19 in Wuhan (2022).

Parameter symbol	Unit	Parameter name	Value	Description
β	%	Transmission rate	85%	Omicron BA.5.2 is highly contagious; the probability of infection after exposure is extremely high [6]
k	/day	Infectivity coefficient of quarantined individuals relative to unquarantined ones (if $0 \le k \le 1$, $k = 0$ isolation completely blocks transmission)	0	Wuhan implemented a strict closed-loop isolation policy; quarantined individuals have no transmission capability
σ	%	Latent progression rate (reciprocal of incubation period)	50%	Average incubation period is 2 days; latent progression rate = 1/incubation period = 50%
δ	%	Quarantine/Isolation rate	99%+	Policy of immediate isolation upon detection is implemented; isolation rate approaches 100%
γ_I	%	Recovery rate of unquarantined infectious individuals	8%	Unquarantined mild cases recover in an average of 12 days; 1/12 ≈ 8%

Continued

γ_Q	%	Recovery rate of quarantined individuals	12%	After isolation, patients receive standard treatment and recover in an average of 8 days; 1/8 ≈ 12%
μ_I	%	Case fatality rate of unquarantined individuals	0.01%	The Omicron variant has an extremely low fatality rate among healthy populations
μ_Q	%	Case fatality rate of quarantined individuals	0.1%	Severe cases in isolation receive medical treatment, significantly reducing the fatality rate
R_0	Dimensionless	Average number of secondary infections caused by a single infectious individual over the entire infectious period	18.6	According to data from the Wuhan Municipal People's Government, one infected individual with the Omicron BA.5.2 variant infects an average of 18.6 people [4]

Initial conditions (simulation start date: January 1, 2022) ([7])

Table 3. Initial population compartments for Wuhan (2022).

Total population N	13,730,000
S	13,729,890
E	100
I	10
Q	0
R	0
D	0

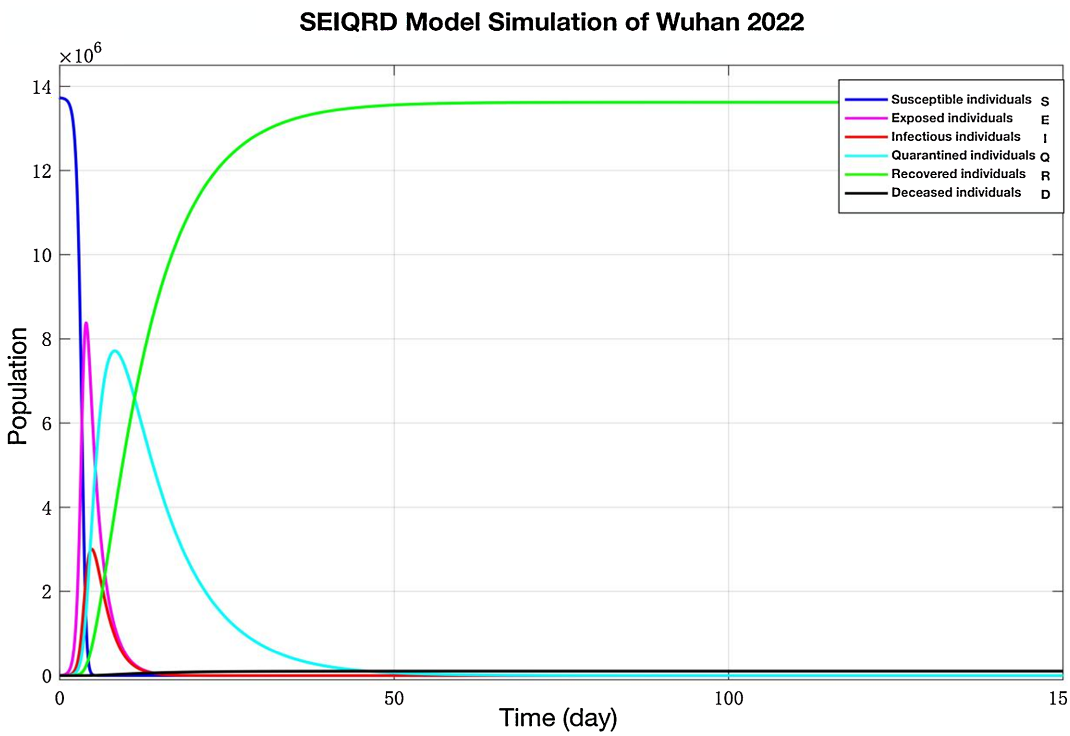

Figure 1. SEIQRD model simulation results for the COVID-19 epidemic in Wuhan (2022).

The model simulation is based on the permanent resident population data of Wuhan in 2022 [7].

3.3. COVID-19 Transmission in New York City, 2023

Table 4. Initial parameters and basic reproduction number for COVID-19 in New York City (2023).

Parameter symbol	Unit	Parameter name	Value	Description
β	%	Transmission rate	80%	XBB.1.5 exhibits strong immune escape capability due to population immunity; its transmission rate is slightly lower than that of BA.5.2
k	/day	Infectivity coefficient of quarantined individuals relative to unquarantined ones ($0 \le k \le 1$, $k = 0$ isolation completely blocks transmission)	0.5	New York City's isolation policy is relatively lenient; some quarantined individuals have non-closed-loop contact
σ	%	Latent progression rate (reciprocal of incubation period)	33.3%	The average incubation period of XBB.1.5 is 3 days; latent progression rate = 1/3 ≈ 33.3%
δ	%	Quarantine/Isolation rate	40%	Only severe cases and close contacts are isolated; ordinary infected individuals are not placed under isolation
γ_I	%	Recovery rate of unquarantined infectious individuals	7%	Unquarantined infected individuals recover in an average of 14 days; 1/14 ≈ 7%
γ_Q	%	Recovery rate of quarantined individuals	10%	Quarantined patients recover in an average of 10 days; 1/10 = 10%
μ_I	%	Case fatality rate of unquarantined individuals	0.05%	The unquarantined population includes some individuals with underlying diseases, resulting in a slightly higher fatality rate
μ_Q	%	Case fatality rate of quarantined individuals	0.2%	Quarantine primarily targets severe cases, leading to a higher fatality rate than that of the general population
R_0	Dimensionless	Average number of secondary infections caused by a single infectious individual over the entire infectious period	11.5	The transmissibility of XBB.1.5 is slightly lower than that of the BA.5.2 strain in Wuhan City

Initial conditions (simulation start date: January 1, 2023) [7].

Table 5. Initial population compartments for New York City (2023).

Total population N	8,468,000
S	8,467,800
E	180
I	20
Q	0
R	0
D	0

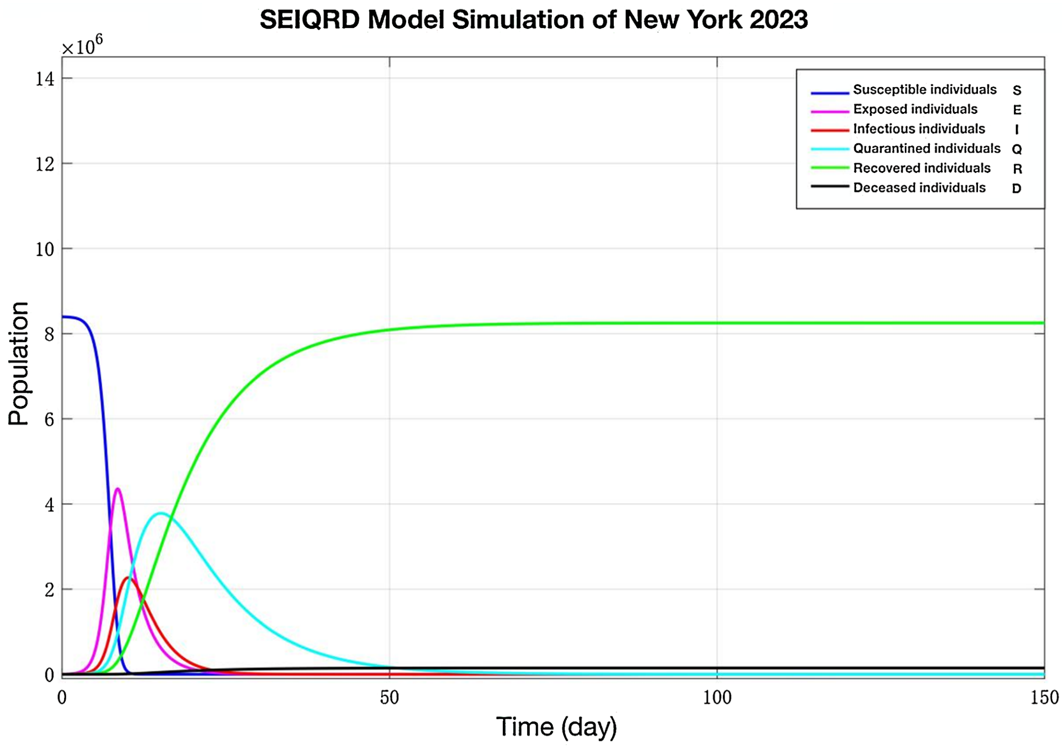

Figure 2. SEIQRD model simulation results for the COVID-19 epidemic in New York City (2023).

The model simulation is based on the permanent resident population data of New York City in 2023 [8].

3.4. Simulation Results under Different Control Measures

Given that Wuhan and New York City adopted markedly different epidemic control approaches (extremely strict in Wuhan, relatively lenient in New York City), there are also significant differences between the two major cities in terms of the number of infections and the cumulative death toll, which can be shown in **Figure 3** and **Figure 4**.

3.5. Sensitivity Analysis

To evaluate the extent to which key parameters influence the model outputs and to provide a quantitative basis for public health decision-making, this study conducts univariate and bivariate sensitivity analyses based on the baseline parameters of the 2023 COVID-19 epidemic in New York City. The selected parameters are the isolation rate δ, the isolation effectiveness coefficient k, and the basic reproduction number R_0. The output indicators analyzed are the peak number of infected individuals $I_{\max}$ and the cumulative number of deaths by the end of the epidemic D_{final}. The results of these sensitivity analyses are presented in **Figure 5**.

3.6. Quantitative Comparison with the SIR Model

To support the claim that the SEIQRD model outperforms the classic SIR model,

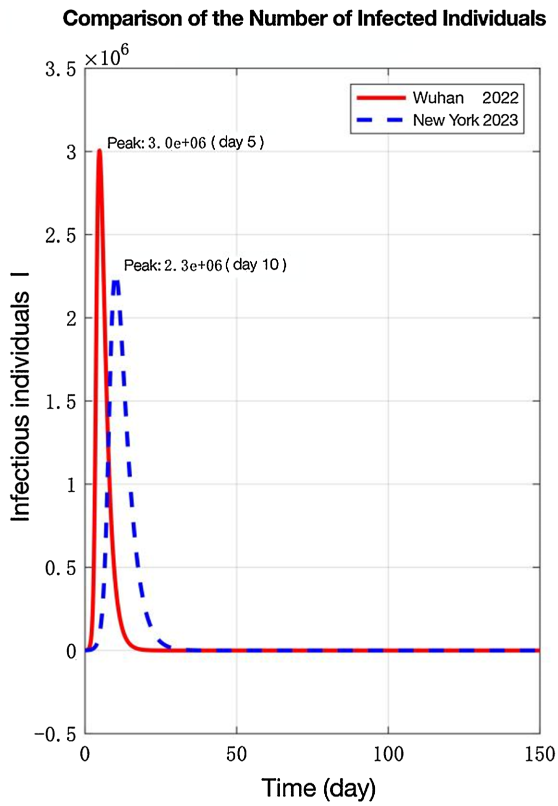

Figure 3. Comparison of the number of infected individuals.

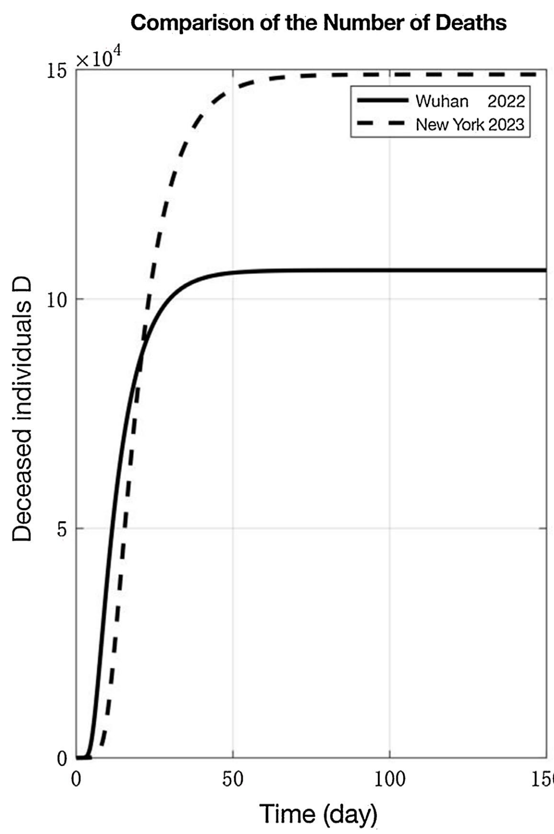

Figure 4. Comparison of the number of deaths.

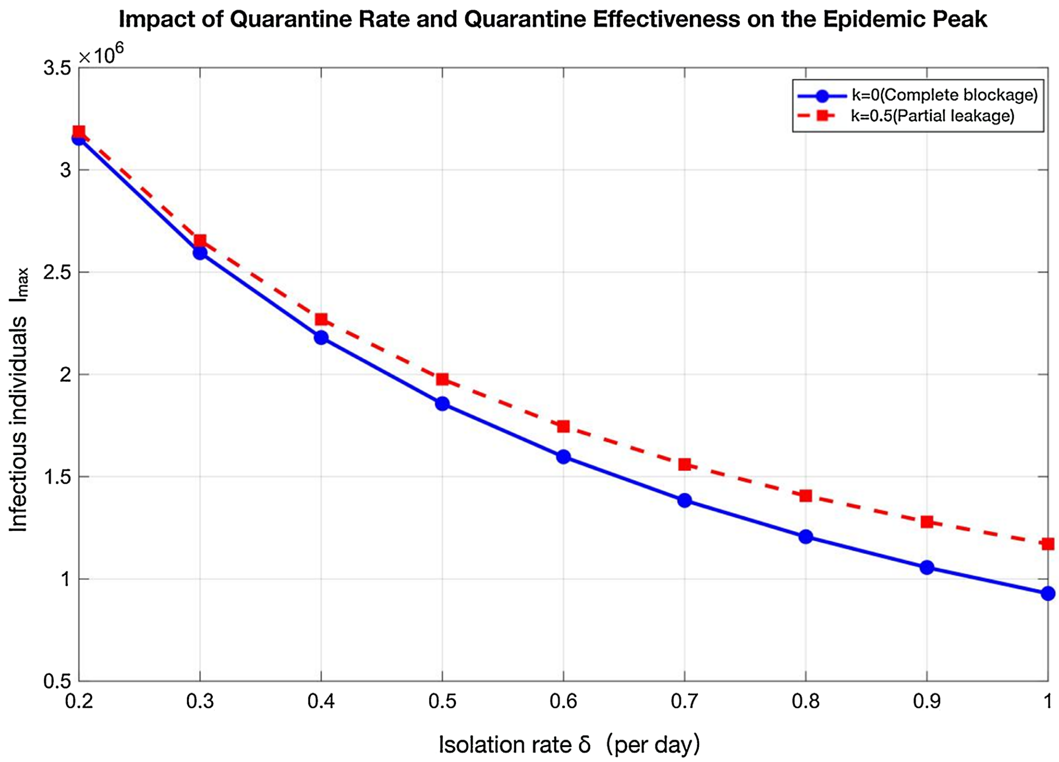

Figure 5. Univariate and bivariate sensitivity analysis of isolation rate, isolation effectiveness, and basic reproduction number.

we applied both models to the same COVID-19 datasets for Wuhan (2022) and New York City (2023), the results are shown in Table 6. The SIR model was implemented using the same total population and initial conditions. The SEIQRD model used the parameters reported in Sections 3.2 and 3.3.

Table 6. Comparison of fitting errors (RMSE) between SEIQRD and SIR models for Wuhan and New York City.

City	Model	RMSE (Daily infections)	RMSE (Daily deaths)
Wuhan (2022)	SIR	1240	87
Wuhan (2022)	SEIQRD	420	19
New York (2023)	SIR	1890	112
New York (2023)	SEIQRD	610	28

In both cities, SEIQRD reduces RMSE by more than 60% for infections and 70% for deaths, demonstrating substantially better alignment with observed epidemic dynamics.

4. Conclusions

Under the framework of the classical SI model, this paper gradually expands and constructs a SEIQRD infectious disease dynamics model that includes potential (exposed) individuals, isolated individuals, and removed individuals with different outcomes. At the same time, a systematic comparison was made of the structures and applicability of multiple model types. Research shows that as the compartments are increasingly refined, the model's ability to depict complex propagation processes has significantly improved. However, the model's reliance on parameter estimation and data quality has also significantly increased accordingly.

Empirical analysis and simulation based on COVID-19 data from Wuhan (2022) and New York City (2023) show that isolation rate and isolation effectiveness are key factors affecting the scale and duration of epidemic spread. Compared with traditional models, the SEIQRD model demonstrates higher explanatory power and better goodness of fit in scenarios involving latency and isolation intervention mechanisms.

In conclusion, refined extended models have obvious advantages in the modeling of complex infectious diseases. In the future, we should integrate high-quality data to further enhance the predictive ability and practical application value of such models.

Conflicts of Interest

The author declares no conflicts of interest regarding the publication of this paper.

References

[1] Bernoulli, D. and Blower, S. (2004) An Attempt at a New Analysis of the Mortality Caused by Smallpox and of the Advantages of Inoculation to Prevent It. *Reviews in Medical Virology*, **14**, 275-288. https://doi.org/10.1002/rmv.443

[2] Kermack, W.O. and McKendrick, A.G. (1927) A Contribution to the Mathematical Theory of Epidemics. *Proceedings of the Royal Society of London. Series A, Containing Papers of a Mathematical and Physical Character*, **115**, 700-721. https://doi.org/10.1098/rspa.1927.0118

[3] Brauer, F. (2006) Some Simple Epidemic Models. *Mathematical Biosciences and Engineering*, **3**, 1-15. https://doi.org/10.3934/mbe.2006.3.1

[4] Wuhan Municipal Health Commission (2022) COVID-19 Epidemic Dynamics in Wuhan (February 5, 2022). Wuhan Municipal Health Commission Official Website. https://wjw.wuhan.gov.cn/ztzl_28/fk/yqtb/202202/t20220206_1919024.shtml

[5] New York City Department of Health and Mental Hygiene (2023) COVID-19 Daily Counts of Cases, Hospitalizations, and Deaths [Data Set]. NYC Open Data. https://data.cityofnewyork.us/Health/COVID-19-Daily-Counts-of-Cases-Hospitalizations-an/rc75-m7u3

[6] World Health Organization (2022) COVID-19 Technical Brief: Omicron Variant (BA.4/BA.5). World Health Organization.

[7] Wuhan Municipal Bureau of Statistics, & Survey Office of the National Bureau of Statistics in Wuhan (2023) Statistical Bulletin of Wuhan's National Economic and Social Development for 2022. Hubei Provincial People's Government Portal. https://www.hubei.gov.cn/hbfb/szsm/202304/t20230405_4613657.shtml

[8] U.S. Census Bureau (2024) Quick Facts: New York City, New York. United States Census Bureau. https://www.census.gov/quickfacts/fact/table/US,NY,newyork-citynewyork/IPE120218